



Cite this: DOI: 10.1039/d0cc02451a

Received 4th April 2020,  
Accepted 5th May 2020

DOI: 10.1039/d0cc02451a

rsc.li/chemcomm

# X-Ray fluorescence microscopy reveals that rhenium(i) tricarbonyl isonitrile complexes remain intact *in vitro*<sup>†</sup>

Chilaluck C. Konkankit,<sup>a</sup> James Lovett,<sup>b</sup> Hugh H. Harris<sup>b</sup> and Justin J. Wilson<sup>\*a</sup>

The complex *fac*-[Re(CO)<sub>3</sub>(dmphen)(*para*-tolylisonitrile)]<sup>+</sup> (**TRIP**), where dmphen = 2,9-dimethyl-1,10-phenanthroline, is an endoplasmic reticulum stress-inducing anticancer agent (A. P. King, S. C. Marker, R. V. Swanda, J. J. Woods, S.-B. Qian and J. J. Wilson, *Chem. – Eur. J.*, 2019, 25, 9206–9210). A second-generation compound *fac*-[Re(CO)<sub>3</sub>(dmphen)(*para*-iodobenzeneisonitrile)]<sup>+</sup> (**I-TRIP**) was synthesized, and its intracellular distribution was investigated using X-ray fluorescence microscopy to show that these complexes are highly stable *in vitro*.

There is an increasing number of reports on the promising *in vitro* and *in vivo* anticancer activity of Re-based compounds due to their high stability, structural diversity, amenability for real-time imaging, and lack of off-site toxicity *in vivo*.<sup>1–19</sup> Among these Re-based drug candidates, complexes containing the Re(i) tricarbonyl Re(CO)<sub>3</sub> core are the most commonly explored for this application. Within this research area, our lab has led several efforts to design and identify Re(CO)<sub>3</sub> compounds as potent chemotherapeutic drug candidates.<sup>20–23</sup> We have also illustrated their ability to operate *in vivo* without inducing toxic side effects, demonstrating the potential of this class of compounds for cancer treatment.<sup>24</sup> Recently, we have identified a tricarbonyl Re isonitrile polypyridyl complex *fac*-[Re(CO)<sub>3</sub>(dmphen)(*para*-tolylisonitrile)]<sup>+</sup>, where dmphen = 2,9-dimethyl-1,10-phenanthroline, called **TRIP**, with promising *in vitro* cytotoxic activity (Fig. 1).<sup>22</sup> **TRIP** was imaged *via* confocal fluorescence microscopy using its photoluminescent triplet metal-to-ligand charge transfer (<sup>3</sup>MLCT) excited state. These results are similar to the first-generation complex, *fac*-[Re(CO)<sub>3</sub>(dmphen)(H<sub>2</sub>O)]<sup>+</sup>, which was also imaged in a similar manner.<sup>20</sup> The ability to detect the emissive <sup>3</sup>MLCT state of these complexes in cells suggests that the dmphen ligand remains bound to the Re center while

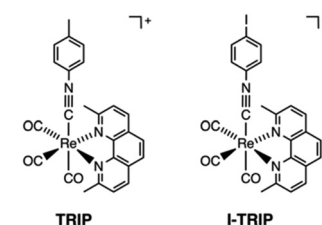


Fig. 1 Structures of the complex cations **TRIP** and **I-TRIP**.

causing cancer cell death. Additionally, **TRIP** induces the accumulation of misfolded proteins, thereby giving rise to endoplasmic reticulum (ER) stress, the unfolded protein response (UPR) pathway, and intrinsic apoptotic cell death. Although the UPR pathway, which is a consequence of ER stress, usually operates in a cytoprotective manner that may result in resistant and more lethal forms of cancer,<sup>25</sup> acute levels of ER stress can overburden the UPR pathway, leading to apoptotic cell death. This cell death pathway has been demonstrated to mediate the *in vitro* cytotoxic activity of several transition metal polypyridyl complexes.<sup>26–31</sup> Because **TRIP** induces this somewhat unusual form of UPR-mediated cancer cell death, we sought to investigate the speciation, namely the stability of the axial ligand, of this compound *in vitro* using synchrotron X-ray fluorescence microscopy (XFM).

XFM is an effective intracellular characterization method that relies on element-specific X-ray fluorescence emissions from core-shell transitions. This technique is highly sensitive and can effectively probe for cellular uptake and intracellular distribution of a wide range of complexes, including metal-based anticancer agents.<sup>32–40</sup> When imaging compounds in cells, this method works best with an exogenous element present in the molecule of interest. To investigate the axial ligand stability of **TRIP** using this method, we utilized a second-generation Re(CO)<sub>3</sub> complex of the formula *fac*-[Re(CO)<sub>3</sub>(dmphen)(I-ICN)]<sup>+</sup>, where I-ICN is *para*-iodobenzeneisonitrile (**I-TRIP**) (Fig. 1). In comparison to **TRIP**, this compound bears an iodo substituent in place of the methyl group on the axial isonitrile ligand. Because I is of low abundance in most *in vitro* cellular systems,<sup>41</sup> the iodo group on **I-TRIP**

<sup>a</sup> Department of Chemistry and Chemical Biology, Cornell University, Ithaca, New York 14853, USA. E-mail: jjw275@cornell.edu

<sup>b</sup> Department of Chemistry, The University of Adelaide, South Australia 5005, Australia

<sup>†</sup> Electronic supplementary information (ESI) available. See DOI: 10.1039/d0cc02451a

provides an additional XFM spectroscopic handle. Using this complex, the axial ligand stability of this class of compounds can be determined by directly comparing the elemental distributions of I and Re in cells. Prior to carrying out XFM analysis, we first sought to characterize the biological activity of **I-TRIP** to determine if the complex operates *via* a similar mechanism of action as the parent compound, **TRIP**.

**TRIP** was synthesized following previously reported methods and verified to be >95% pure by  $^1\text{H}$  NMR spectroscopy and reversed-phase HPLC (RP-HPLC). **I-TRIP** was similarly synthesized using the I-bearing isonitrile ligand (Fig. S1 and S2, ESI $^\dagger$ ) and was fully characterized with  $^1\text{H}$  NMR spectroscopy (Fig. S3, ESI $^\dagger$ ), UV-Vis spectroscopy (Fig. S4, ESI $^\dagger$ ), Fourier transform infrared (FTIR) spectroscopy (Fig. S5, ESI $^\dagger$ ), and electrospray ionization mass spectrometry (ESI-MS) (Fig. S6, ESI $^\dagger$ ). The purity of this compound was verified to be greater than 95% *via* RP-HPLC (Fig. S7, ESI $^\dagger$ ) and elemental analysis. With **I-TRIP** in hand, its cytotoxicity was evaluated and compared to that of **TRIP** in HeLa cervical cancer cells *via* the thiazolyl blue tetrazolium bromide (MTT) assay (Table S1 and Fig. S8, ESI $^\dagger$ ). The 50% growth inhibitory concentration ( $\text{IC}_{50}$ ) value of **I-TRIP** in this cell line is 3.3  $\mu\text{M}$ , whereas this value is 1.8  $\mu\text{M}$  for the parent compound, **TRIP**. Accounting for experimental error in each of these measurements, the difference between these values is not statistically significant ( $p > 0.05$ ), thus indicating that both compounds exhibit similar cytotoxic activities in HeLa cells. Having demonstrated that these complexes possess comparable potencies, we next evaluated whether they operate *via* similar mechanisms of action.

**TRIP** induces cancer cell death in a manner that is accompanied by ER stress, the UPR pathway, and inhibition of protein translation.<sup>22</sup> To verify that **I-TRIP** is an appropriate model for **TRIP** that causes cell death in a similar fashion, we carried out detailed biological mechanistic studies for this compound. Similar to **TRIP**, **I-TRIP** kills cancer cells *via* caspase-dependent apoptosis. This conclusion is supported by the fact that the cytotoxic activity of **I-TRIP** is diminished in the presence of the pan-caspase inhibitor, Z-VAD-FMK (Fig. 2a). Furthermore, the cytotoxicity of **I-TRIP** is enhanced in the presence of the compound salubrinal (Fig. 2b), marking another similarity to **TRIP**. Salubrinal inhibits dephosphorylation of the protein eukaryotic translation initiation factor  $2\alpha$  (eIF2 $\alpha$ ), which is intimately involved in the UPR pathway and ER stress.<sup>42–44</sup> The synergistic effects of **I-TRIP** with salubrinal are consistent with previous results for **TRIP**, and they indicate that this new Re complex also induces ER stress. In further support of this mechanistic similarity between **TRIP** and **I-TRIP**, western blotting was performed to determine the expression level of the proapoptotic protein, CHOP, which is induced *via* ER stress.<sup>45,46</sup> The blot depicts the induced expression of CHOP after treating with the Re complexes, verifying that **I-TRIP** induces apoptotic cell death *via* ER stress in a similar fashion to **TRIP** (Fig. 2c). As a final validation that **TRIP** and **I-TRIP** follow similar biological mechanisms of action, a puromycin incorporation assay was used to investigate the abilities of these compounds to inhibit protein translation.<sup>47</sup> Puromycin is a tyrosine and phenylalanine mimic that is incorporated into proteins during translation, providing a quantifiable marker for this process which can be detected by

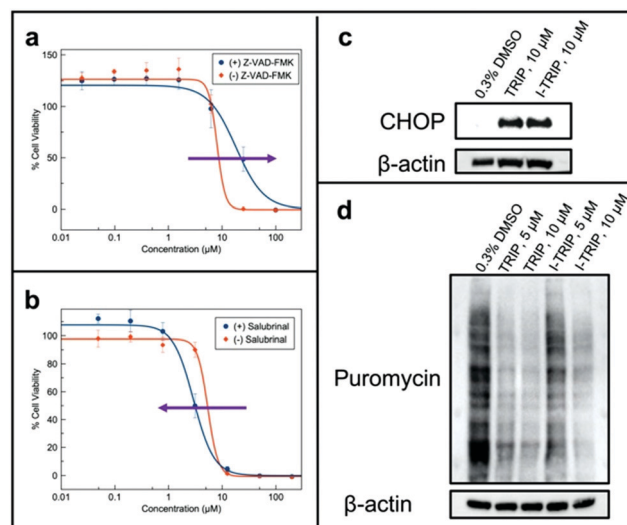
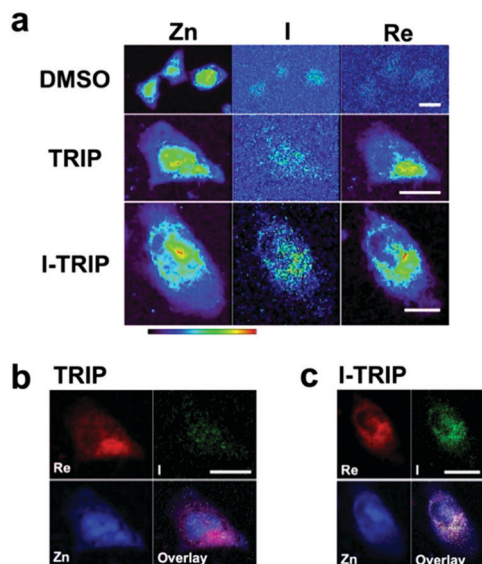


Fig. 2 Compound **I-TRIP** was examined for its biological activity. Dose-response curves in the presence of (a) the pan-caspase inhibitor, Z-VAD-FMK, and (b) the ER stress modulator, salubrinal. (c) Western blot for CHOP expression of HeLa cell lysates treated with DMSO (0.3% v/v), **TRIP** (10  $\mu\text{M}$ ), or **I-TRIP** (10  $\mu\text{M}$ ) for 24 h. (d) Western blot for puromycin incorporation of HeLa cell lysates treated with DMSO (0.3% v/v), **TRIP** (5 and 10  $\mu\text{M}$ ), or **I-TRIP** (5 and 10  $\mu\text{M}$ ) for 24 h. After the 24 h incubation, puromycin (60  $\mu\text{M}$ ) was added for an additional 10 min.

specific high-affinity antibodies *via* western blot.<sup>48,49</sup> As shown in Fig. 2d, both **TRIP** and **I-TRIP** significantly reduce incorporation of puromycin into the proteome, indicating that these agents effectively inhibit protein translation. Taken together, these biological studies demonstrate that **I-TRIP** causes similar *in vitro* biological effects as **TRIP**, thus indicating that alteration of the isonitrile substituents within this class of compounds does not change their mechanisms of action.

Having demonstrated that **I-TRIP** operates in a similar manner as **TRIP**, we next sought to use the elemental signature of the I in its axial ligand to probe its stability in cells *via* XFM. Our approach follows that of a previously reported study involving a  $\text{Re}(\text{CO})_3$  complex bearing an axial I-containing tetrazolate ligand.<sup>10</sup> In this previous study, the compound,  $\text{fac}[\text{Re}(\text{CO})_3(\text{phen})\text{L}]$ , where phen = 1,10-phenanthroline and L = 5-(4-iodophenyl)-tetrazolate, was imaged in cells by XFM to show that Re and I elemental maps were coincident with one another, signifying that the axial ligand remains bound under these conditions. Inspired by this study, we explored the elemental distributions of Re and I in HeLa cells treated with **TRIP** and **I-TRIP** using XFM (Fig. 3a–c). Both **TRIP** and **I-TRIP** give rise to detectable Re elemental maps, demonstrating that these compounds can effectively enter cells. In comparison to both vehicle-treated and **TRIP**-treated samples, cells exposed to **I-TRIP** displayed detectable X-ray emissions matching the edge energy of I. We note that the I distribution maps appear coarser and less bright than the Re maps. This feature is due to the lower energy L edge lines (4.5 keV) of I compared to Re (10 keV), which gives rise to photons with less penetrating capability and thus poorer detection efficiency. Despite the difference in L edge intensities, the colocalization of the Re and I signal is



**Fig. 3** (a) XFM elemental distribution maps of HeLa cervical cancer cells treated with DMSO (0.06% v/v), 2  $\mu$ M **TRIP**, or 3  $\mu$ M **I-TRIP**. Correlation analysis on the alignment of Re, I, and Zn distribution maps for (b) **TRIP** and (c) **I-TRIP**. Scale bar = 20  $\mu$ m.

strong, as reflected by a Pearson's correlation coefficient of 0.684 (Fig. 3b, c and Table S2, ESI†). The colocalization of these two elements indicates that the axial isonitrile ligand remains bound to the Re center in the cellular setting. These results are consistent with the XFM study on the *fac*-[Re(CO)<sub>3</sub>(phen)L] compound discussed above. Thus, in a more general sense, some types of axial ligands on such Re(CO)<sub>3</sub> complexes appear to be stable. In addition to mapping Re and I, we also imaged Zn, P, Ca, and S to help our assessment of compound localization (Fig. S9–S11, ESI†). Comparison of the Re elemental maps with those of these endogenous elements, however, revealed no significant colocalization and no appreciable accumulation in the nucleus. Taken together, these results demonstrate that XFM is a useful tool for imaging Re-based complexes and this class of Re isonitrile compounds likely remains intact upon inducing cancer cell death.

In conclusion, the I-containing complex, **I-TRIP**, was synthesized and evaluated as a surrogate for **TRIP** to assess the axial ligand stability of this class of compounds. We confirmed that alteration of the axial isonitrile substituents does not yield a change in the mechanisms of action, validating the use of **I-TRIP** for these purposes. The ability to image the I component on the axial ligand and the Re center directly by XFM enabled us to see that these elements colocalize in cells, indicating that the axial ligand of these Re isonitrile compounds is stable. The promising biological activities and novel mechanisms of action of the **TRIP** and **I-TRIP** complexes further supports the ongoing investigation of this class of compounds as anticancer agents. Knowing now that the axial isonitrile does not act as a leaving group, rational structural modifications to these compounds can be applied to enhance their anticancer activities.

This research was supported by the College of Arts and Sciences at Cornell University, the Cornell Technology Licensing

Office Cornell Technology Acceleration and Maturation (CTAM) fund, and by the Office of the Assistant Secretary of Defense for Health Affairs through the Ovarian Cancer Research Program under award no. W81XWH-17-1-0097. This work made use of the NMR facility at Cornell University, which is in-part supported by the NSF under award number CHE-1531632. This research used resources of the Advanced Photon Source, a U.S. Department of Energy (DOE) Office of Science User Facility operated for the DOE Office of Science by Argonne National Laboratory under Contract No. DE-AC02-06CH11357. Travel funding for Prof. Hugh Harris and Mr. James Lovett to perform experiments at the Advanced Photon Source was provided by the International Synchrotron Access Program (ISAP) managed by the Australian Synchrotron, part of ANSTO, funded by the Australian Government. We thank Prof. Jeremy Baskin for allowing us to use their confocal fluorescence microscope, and Dr. Sierra Marker is thanked for her assistance with some of these studies. We also thank Prof. Hening Lin for allowing us to use their Bio-Rad ChemiDoc MP imaging system for western blots.

## Conflicts of interest

The authors declare no competing financial interests.

## References

- 1 A. Leonidova and G. Gasser, *ACS Chem. Biol.*, 2014, **9**, 2180–2193.
- 2 L. C.-C. Lee, K.-K. Leung and K. K.-W. Lo, *Dalton Trans.*, 2017, **46**, 16357–16380.
- 3 K. Suntharalingam, S. G. Awuah, P. M. Bruno, T. C. Johnstone, F. Wang, W. Lin, Y.-R. Zheng, J. E. Page, M. T. Hemann and S. J. Lippard, *J. Am. Chem. Soc.*, 2015, **137**, 2967–2974.
- 4 N. I. Shtemenko, P. Collery and A. V. Shtemenko, *Metal Ions in Biology and Medicine*, John Libbey Eurotext, Paris, 2006, pp. 374–378.
- 5 N. I. Shtemenko, H. T. Chifotides, K. V. Domasevitch, A. A. Golichenko, S. A. Babiy, Z. Li, K. V. Paramonova, A. V. Shtemenko and K. R. Dunbar, *J. Inorg. Biochem.*, 2013, **129**, 127–134.
- 6 Z. Li, N. I. Shtemenko, D. Y. Yegorova, S. O. Babiy, A. J. Brown, T. Yang, A. V. Shtemenko and K. R. Dunbar, *J. Liposome Res.*, 2015, **25**, 78–87.
- 7 N. I. Shtemenko, P. Collery and A. V. Shtemenko, *Anticancer Res.*, 2007, **27**, 2487–2492.
- 8 A. V. Shtemenko, P. Collery, N. I. Shtemenko, K. V. Domasevitch, E. D. Zabitskaya and A. A. Golichenko, *Dalton Trans.*, 2009, 5132–5136.
- 9 P. Collery, D. Desmaele and V. Veena, *Curr. Pharm. Des.*, 2019, **25**, 1–17.
- 10 J. L. Wedding, H. H. Harris, C. A. Bader, S. E. Plush, R. Mak, M. Massi, D. A. Brooks, B. Lai, S. Vogt, M. V. Werrett, P. V. Simpson, B. W. Skelton and S. Stagni, *Metallomics*, 2017, **9**, 382–390.
- 11 E. B. Bauer, A. A. Haase, R. M. Reich, D. C. Crans and F. E. Kühn, *Coord. Chem. Rev.*, 2019, **393**, 79–117.
- 12 F. Zobi, O. Blacque, R. K. O. Sigel and R. Alberto, *Inorg. Chem.*, 2007, **46**, 10458–10460.
- 13 A. Egli, K. Hegetschweiler, R. Alberto, U. Abram, R. Schibli, R. Hedinger, V. Gramlich, R. Kissner and P. A. Schubiger, *Organometallics*, 1997, **16**, 1833–1840.
- 14 F. Zobi, B. Spingler and R. Alberto, *ChemBioChem*, 2005, **6**, 1397–1405.
- 15 S. Imstepf, V. Pierroz, R. Rubbiani, M. Felber, T. Fox, G. Gasser and R. Alberto, *Angew. Chem., Int. Ed.*, 2016, **55**, 2792–2795.
- 16 A. Leonidova, V. Pierroz, L. A. Adams, N. Barlow, S. Ferrari, B. Graham and G. Gasser, *ACS Med. Chem. Lett.*, 2014, **5**, 809–814.
- 17 S. Imstepf, V. Pierroz, P. Rapsinho, M. Felber, T. Fox, C. Fernandes, G. Gasser, I. R. Santos and R. Alberto, *Dalton Trans.*, 2016, **45**, 13025–13033.
- 18 C. C. Konkankit, S. C. Marker, K. M. Knopf and J. J. Wilson, *Dalton Trans.*, 2018, **47**, 9934–9974.

- 19 M. S. Capper, H. Packman and M. Rehkämper, *ChemBioChem*, 2020, DOI: 10.1002/cbic.202000117.
- 20 K. M. Knopf, B. L. Murphy, S. N. MacMillan, J. M. Baskin, M. P. Barr, E. Boros and J. J. Wilson, *J. Am. Chem. Soc.*, 2017, **139**, 14302–14314.
- 21 S. C. Marker, S. N. MacMillan, W. R. Zipfel, Z. Li, P. C. Ford and J. J. Wilson, *Inorg. Chem.*, 2018, **57**, 1311–1331.
- 22 A. P. King, S. C. Marker, R. V. Swanda, J. J. Woods, S.-B. Qian and J. J. Wilson, *Chem. – Eur. J.*, 2019, **25**, 9206–9210.
- 23 C. C. Konkankit, B. A. Vaughn, S. N. MacMillan, E. Boros and J. J. Wilson, *Inorg. Chem.*, 2019, **58**, 3895–3909.
- 24 C. C. Konkankit, A. P. King, K. M. Knopf, T. L. Southard and J. J. Wilson, *ACS Med. Chem. Lett.*, 2019, **10**, 822–827.
- 25 M. J. Mann and L. M. Hendershot, *Cancer Biol. Ther.*, 2006, **5**, 736–740.
- 26 K. Suntharalingam, T. C. Johnstone, P. M. Bruno, W. Lin, M. T. Hemann and S. J. Lippard, *J. Am. Chem. Soc.*, 2013, **135**, 14060–14063.
- 27 J. S. Nam, M.-G. Kang, J. Kang, S.-Y. Park, S. J. C. Lee, H.-T. Kim, J. K. Seo, O.-H. Kwon, M. H. Lim, H.-W. Rhee and T.-H. Kwon, *J. Am. Chem. Soc.*, 2016, **138**, 10968–10977.
- 28 X. Meng, M. L. Leyva, M. Jenny, I. Gross, S. Benosman, B. Fricker, S. Harlepp, P. Hébraud, A. Boos, P. Wlosik, P. Bischoff, C. Sirlin, M. Pfeffer, J.-P. Loeffler and C. Gaiddon, *Cancer Res.*, 2009, **69**, 5458–5466.
- 29 T. Zou, C.-N. Lok, Y. M. E. Fung and C.-M. Che, *Chem. Commun.*, 2013, **49**, 5423–5425.
- 30 R. Cao, J. Jia, X. Ma, M. Zhou and H. Fei, *J. Med. Chem.*, 2013, **56**, 3636–3644.
- 31 J. Pracharova, G. Vigueras, V. Novohradsky, N. Cutillas, C. Janiak, H. Kostrhunova, J. Kasparkova, J. Ruiz and V. Brabec, *Chem. – Eur. J.*, 2018, **24**, 4607–4619.
- 32 A. E. Garcia, B. Lai, S. G. Gopinathan, H. H. Harris, C. S. Shemanko and F. Jalilehvand, *Chem. Commun.*, 2019, **55**, 8223–8226.
- 33 D. E. Morrison, J. B. Aitken, M. D. de Jonge, J. A. Ioppolo, H. H. Harris and L. M. Rendina, *Chem. Commun.*, 2014, **50**, 2252–2254.
- 34 H. H. Harris, A. Levina, C. T. Dillon, I. Mulyani, B. Lai, Z. Cai and P. A. Lay, *J. Biol. Inorg. Chem.*, 2005, **10**, 105–118.
- 35 K. L. Munro, A. Mariana, A. I. Klavins, A. J. Foster, B. Lai, S. Vogt, Z. Cai, H. H. Harris and C. T. Dillon, *Chem. Res. Toxicol.*, 2008, **21**, 1760–1769.
- 36 K. J. Davis, J. A. Carrall, B. Lai, J. R. Aldrich-Wright, S. F. Ralph and C. T. Dillon, *Dalton Trans.*, 2012, **41**, 9417–9426.
- 37 F. Fus, Y. Yang, H. Z. S. Lee, S. Top, M. Carriere, A. Bouron, A. Pacureanu, J. C. da Silva, M. Salmain, A. Vessièrès, P. Cloetens, G. Jaouen and S. Bohic, *Angew. Chem., Int. Ed.*, 2019, **58**, 3461–3465.
- 38 J. B. Aitken, S. Antony, C. M. Weekley, B. Lai, L. Spiccia and H. H. Harris, *Metallomics*, 2012, **4**, 1051–1056.
- 39 M. J. Pushie, I. J. Pickering, M. Korbas, M. J. Hackett and G. N. George, *Chem. Rev.*, 2014, **114**, 8499–8541.
- 40 J. Markham, J. Liang, A. Levina, R. Mak, B. Johannessen, P. Kappen, C. J. Glover, B. Lai, S. Vogt and P. A. Lay, *Eur. J. Inorg. Chem.*, 2017, 1812–1823.
- 41 P. T. Bhattacharya, S. R. Misra and M. Hussain, *Scientifica*, 2016, **2016**, 5464373.
- 42 J. B. DuRose, D. Scheuner, R. J. Kaufman, L. I. Rothblum and M. Niwa, *Mol. Cell. Biol.*, 2009, **29**, 4295–4307.
- 43 K. Pakos-Zebrucka, I. Koryga, K. Mnich, M. Ljujic, A. Samali and A. M. Gorman, *EMBO Rep.*, 2016, **17**, 1374–1395.
- 44 M. Boyce, K. F. Bryant, C. Jousse, K. Long, H. P. Harding, D. Scheuner, R. J. Kaufman, D. Ma, D. M. Coen, D. Ron and J. Yuan, *Science*, 2005, **307**, 935–939.
- 45 H. Hu, M. Tian, C. Ding and S. Yu, *Front. Immunol.*, 2019, **9**, 3083.
- 46 Y. Li, Y. Guo, J. Tang, J. Jiang and Z. Chen, *Acta Biochim. Biophys. Sin.*, 2014, **46**, 629–640.
- 47 S. R. Kimball, *Int. J. Biochem. Cell Biol.*, 1999, **31**, 25–29.
- 48 H. P. Yockey, in *Medical Biochemistry*, ed. L. Versteeg-Buschman, Elsevier Inc., London, United Kingdom, 2017, pp. 493–524.
- 49 E. K. Schmidt, G. Clavarino, M. Ceppi and P. Pierre, *Nat. Methods*, 2009, **6**, 275–277.